Supporting Information

Electrochemical Upcycling of PET to Value-Added Chemicals via Amorphous–Crystalline Interface Engineering

Jinyong Sun,[†a] Yuxiao Wang,[†a] Shuixing Dai,[*a] Arafat Toghan,[*b] Minghua Huang[a]

Preparation of NiCo-LDH/NF

The NiCo-LDH/NF precursor was synthesized through a facile one-step hydrothermal method. In a typical procedure, 3 mmol of $Ni(NO_3)_2·6H_2O$, 6 mmol of $Co(NO_3)_2·6H_2O$, and 20 mmol of urea were dissolved in a mixed solvent consisting of 50 mL anhydrous ethanol and 10 mL deionized water under vigorous stirring to form a homogeneous pink solution. The resulting solution, together with a pretreated nickel foam (NF, 2 × 4 cm), was transferred into a Teflon-lined stainless-steel autoclave and maintained at 120 °C for 6 h. After naturally cooling to room temperature, the obtained NiCo-LDH/NF precursor was repeatedly rinsed with deionized water and anhydrous ethanol, followed by vacuum drying for further use.

Preparation of $NiCo_2O_4$/NF

The $NiCo_2O_4$/NF catalyst was obtained by calcination of the NiCo-LDH/NF precursor. Specifically, NiCo-LDH/NF precursor was placed at the center of a quartz boat and heated in a tubular furnace under an air atmosphere. The temperature was increased to 400 °C at a rate of 2 $°C·min^{-1}$ and maintained for 2 h. After cooling to room temperature, the $NiCo_2O_4$/NF was obtained.

Preparation of NiCu-LDH/$NiCo_2O_4$/NF

NiCu-LDH/$NiCo_2O_4$/NF was fabricated via an electrochemical deposition technique. A mixed electrolyte solution containing 0.1 M $Ni(NO_3)_2·6H_2O$ and 0.05 M $Cu(NO_3)_2·3H_2O$ was prepared in 50 mL deionized water. Electrodeposition was performed using a conventional three-electrode configuration, where $NiCo_2O_4$/NF served as the working electrode, a platinum wire as the counter electrode, and an

Ag/AgCl electrode as the reference electrode. The deposition was conducted at a constant potential of –1.0 V (vs. Ag/AgCl) for 90 s at room temperature. The obtained electrode was rinsed thoroughly with deionized water and anhydrous ethanol, followed by drying at 60 °C to yield the target NiCu-LDH/$NiCo_2O_4$/NF catalyst.

Preparation of NiCu-LDH/NF Catalyst

The NiCu-LDH/NF catalyst was prepared using the same electrodeposition procedure as described above for NiCu-LDH/$NiCo_2O_4$/NF, except that bare NF was employed as the working electrode instead of $NiCo_2O_4$/NF.

Characterizations

Scanning electron microscopy (SEM) images were acquired using a TESCAN MIRA LMS operated at an accelerating voltage of 15 kV. Transmission electron microscopy (TEM), high-resolution TEM (HRTEM), and selected area electron diffraction (SAED) analyses were carried out on an FEI Tecnai G2 F20 microscope operating at 200 kV. The crystalline structures of the samples were analyzed by X-ray diffraction (XRD) on a Bruker D8 Advance diffractometer equipped with Cu Kα radiation (λ = 1.5406 Å). The surface chemical states were examined using X-ray photoelectron spectroscopy (XPS, Thermo Scientific K-Alpha). Ultraviolet photoelectron spectroscopy (UPS) measurements were conducted on a Thermo ESCALAB Xi+ instrument to determine the work function and valence band structure.

Electrochemical Measurement

All electrochemical measurements were carried out on a CHI 660E electrochemical workstation using a standard three-electrode configuration. The prepared catalysts, with a geometric area of 0.5 × 1 cm^2, were directly employed as the working electrode, while a polished graphite rod and a Hg/HgO electrode served as the counter and reference electrodes, respectively. Linear sweep voltammetry (LSV) was performed at a scan rate of 5 $mV \cdot s^{-1}$, with 80% iR compensation applied for the ethylene glycol oxidation reaction (EGOR) and 95% iR compensation for the hydrogen evolution reaction (HER). All measured potentials were converted to the reversible hydrogen electrode (RHE) scale according to the equation: $E_{RHE} = E_{Hg/HgO} + 0.059 \times pH + 0.098$. Tafel plots were constructed by fitting the linear region of the overpotential

(η) versus the logarithm of current density (log j) according to the Tafel equation: $\eta = b \log(j) + a$, where b represents the Tafel slope. The electrochemically active surface area (ECSA) was calculated as $ECSA = C_{dl} / C_s \times A$, where C_s is the specific capacitance of the electrode (0.04 mF cm^{-2}), and A represents the geometric surface area of the electrode (0.5 cm^2). The value of C_{dl} was extracted by performing cyclic voltammetry (CV) in the non-Faradaic potential region at various scan rates ranging from 10 to 50 mV s^{-1}.

Pretreatment of PET Hydrolysate

A total of 31.5 g of dried polyethylene terephthalate (PET, CB102, 300 mesh) powder was immersed in 500 mL of 2 M KOH aqueous solution in a flask and heated at 80 °C for 18 h with continuous stirring on a hotplate.

Product Analysis

The liquid products of the EGOR were analyzed and quantified using high-performance liquid chromatography (HPLC, Waters e2695), employing 5 mM H_2SO_4 aqueous solution as the mobile phase at a flow rate of 0.5 mL·min^{-1}. The Faradaic efficiency (FE) and formate (FA) productivity were calculated according to the following equations:

$$FE\ (\%) = \frac{\text{mol of formed product}}{\text{total charge passed} / (n \times F)} \times 100\%$$

$$FA\ \text{productivity}\ (\text{mmol cm}^{-2}\ \text{h}^{-1}) = \frac{\text{mmol of formed formate}}{\text{anode area} / \text{reaction time}}$$

Where n is the electron transfer numbers of each formed product, for glycolic acid, n = 4 and for FA, n = 3. F is Faraday constant (96485 C mol^{-1}).

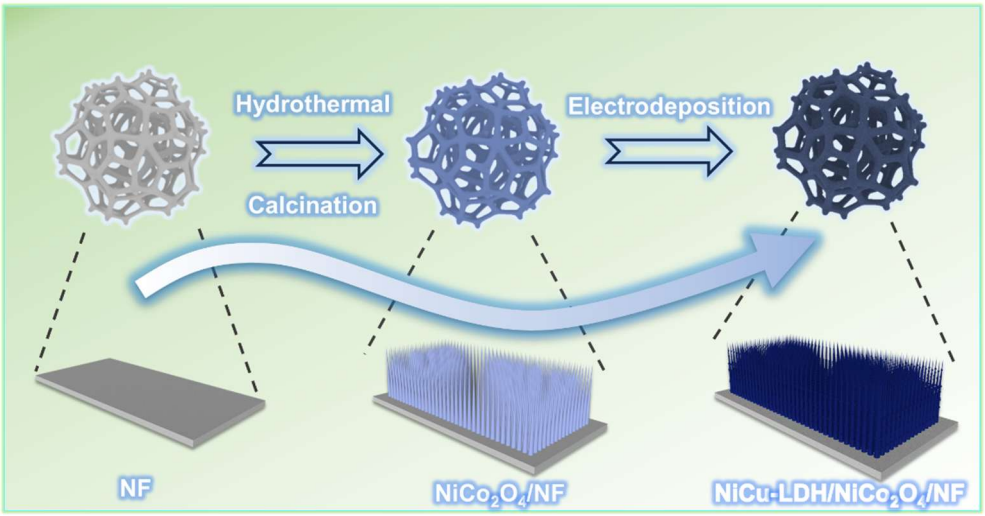

Fig. S1 NiCu-LDH/$NiCo_2O_4$/NF reaction flowchart.

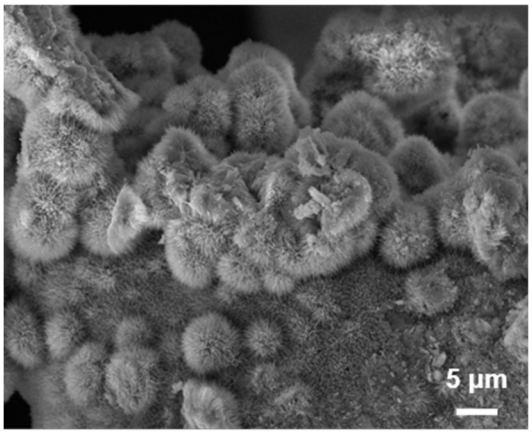

Fig. S2 SEM images of NiCo-LDH/NF.

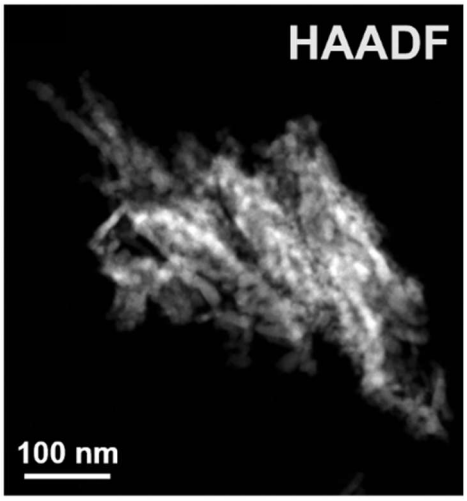

Fig. S3 High angle annular dark-field (HAADF) image of NiCu-LDH/$NiCo_2O_4$/NF.

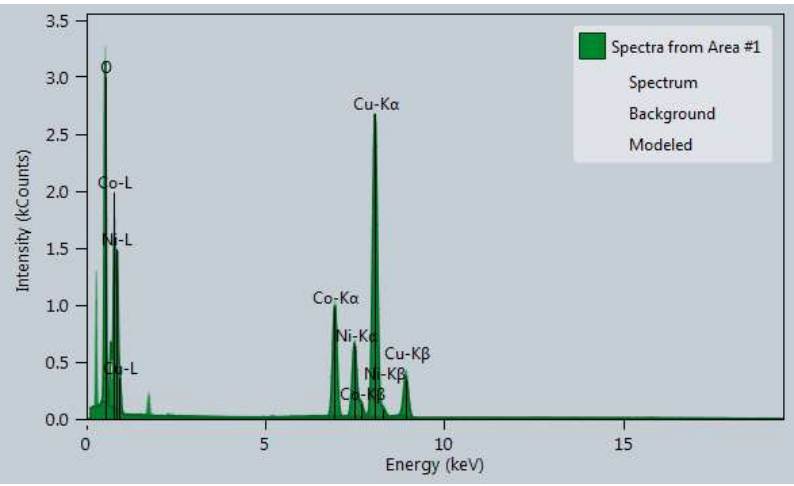

Fig. S4 The EDS pattern of NiCu-LDH/$NiCo_2O_4$/NF.

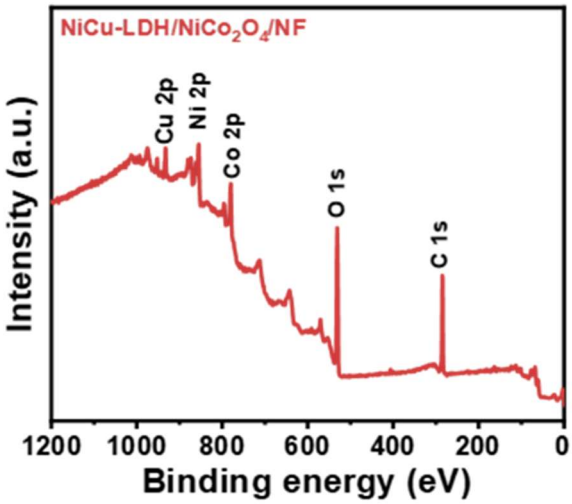

Fig. S5 XPS survey spectra of NiCu-LDH/$NiCo_2O_4$/NF.

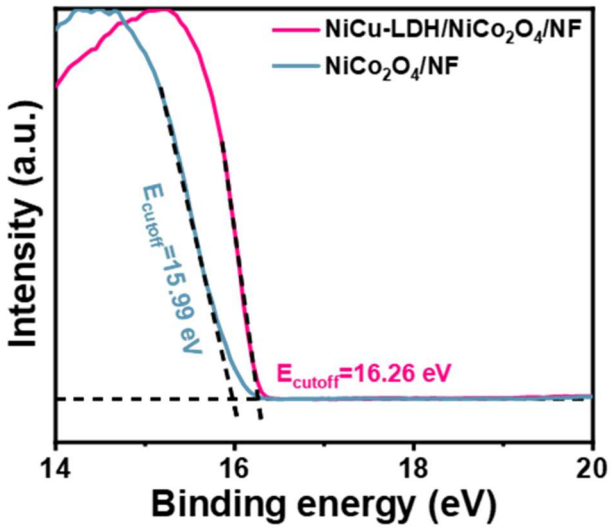

Fig. S6 UPS survey spectra of NiCu-LDH/$NiCo_2O_4$/NF.

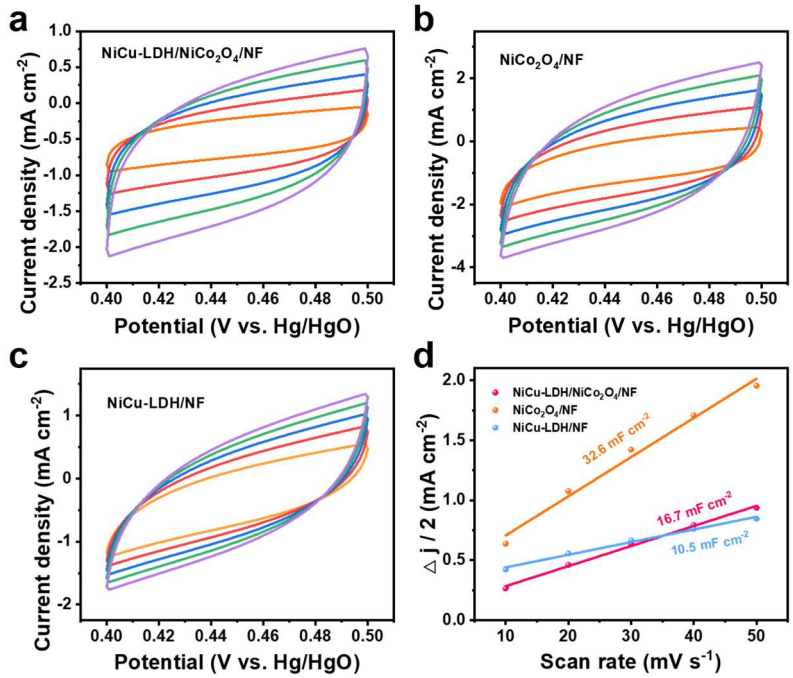

Fig. S7 CV recorded for (a) NiCu-LDH/$NiCo_2O_4$/NF, (b) $NiCo_2O_4$/NF and (c) NiCu-LDH /NF at various scan rates. (d) C_{dl} values of above catalysts.

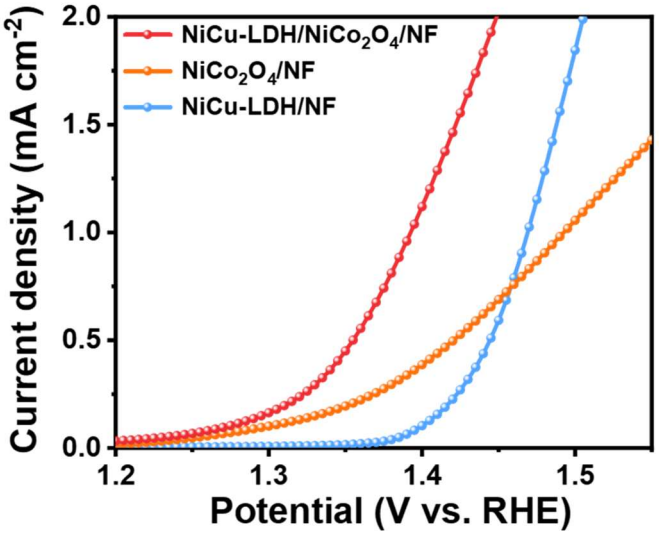

Fig. S8 LSV curves of different catalysts after normalization by ECSA.

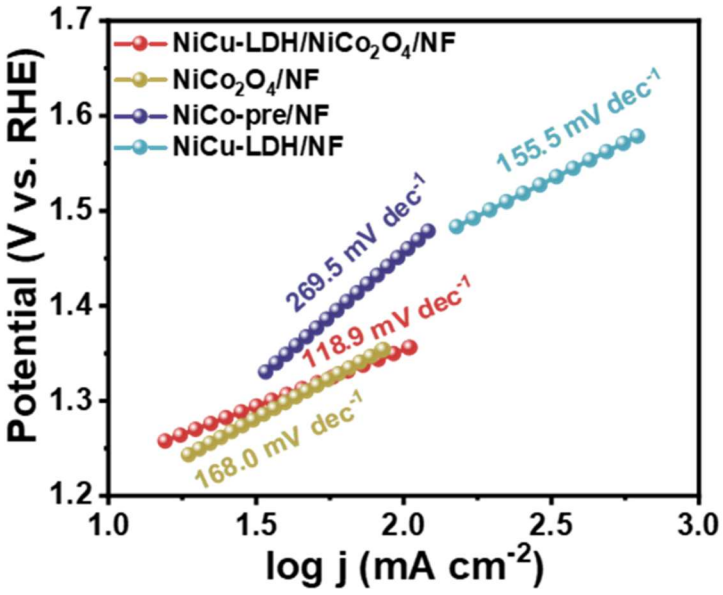

Fig. S9 Tafel plots of different catalysts.

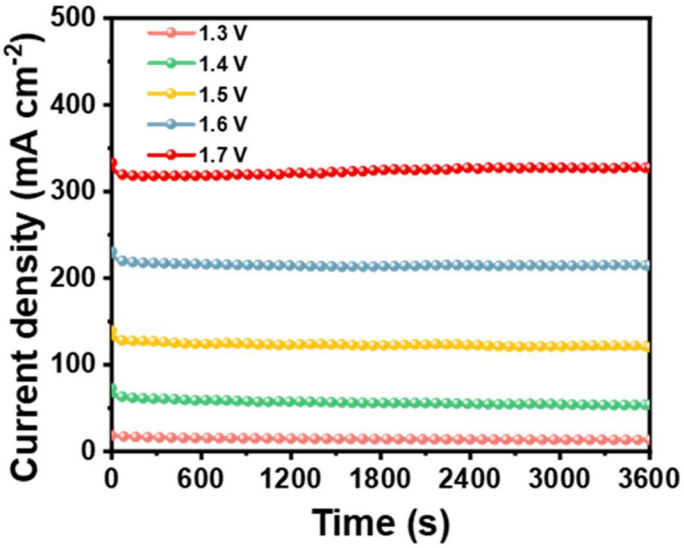

Fig. S10 Chronoamperometric i–t curves of EGOR on NiCu-LDH/$NiCo_2O_4$/NF at different applied potentials.

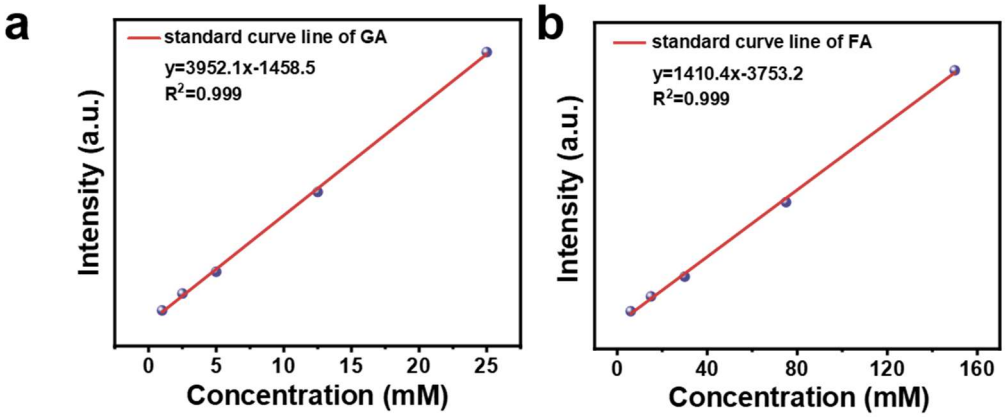

Fig. S11 HPLC calibration curves of (a) GA and (b) FA.

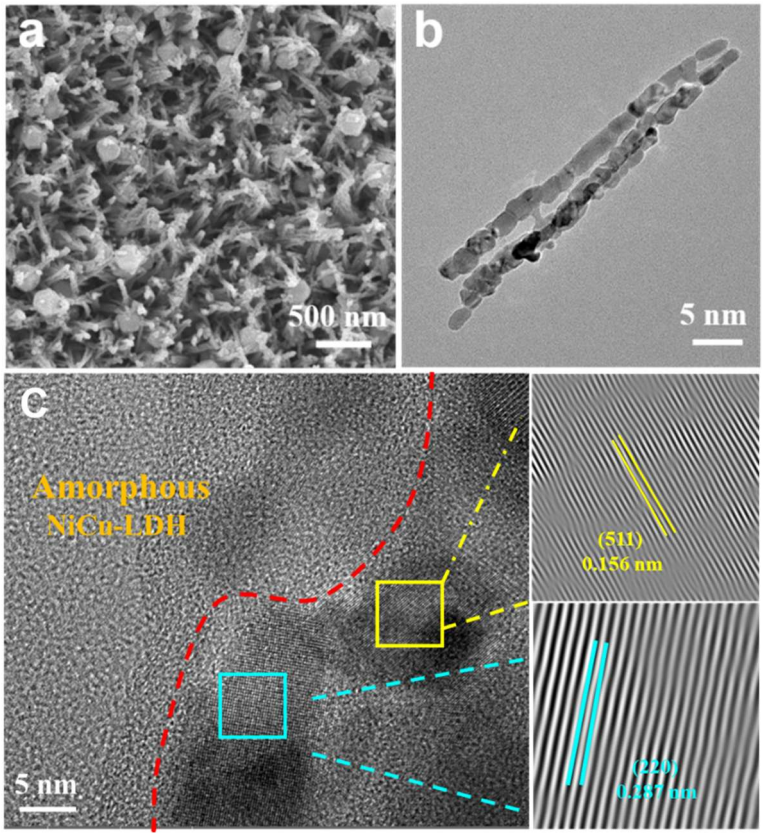

Fig. S12 (a) SEM image, (b) TEM image and (c) HRTEM images of NiCu-LDH/$NiCo_2O_4$/NF after EGOR.

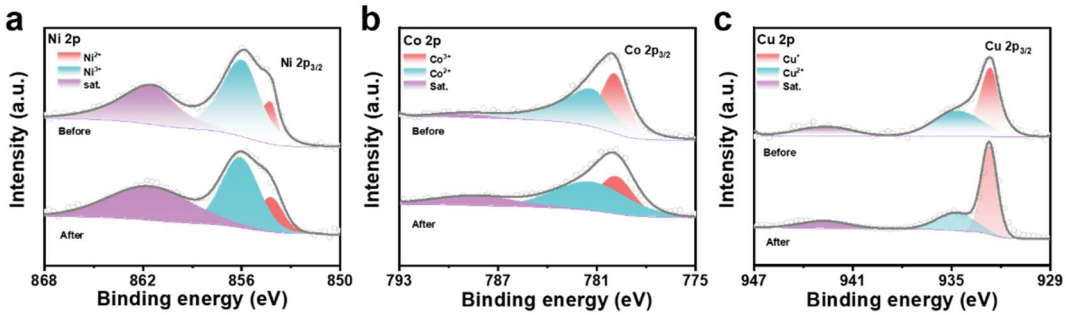

Fig. S13 High-resolution XPS spectra of (a) Ni 2p, (b) Co 2p, and (c) Cu 2p for NiCu-LDH/$NiCo_2O_4$/NF before and after EGOR.

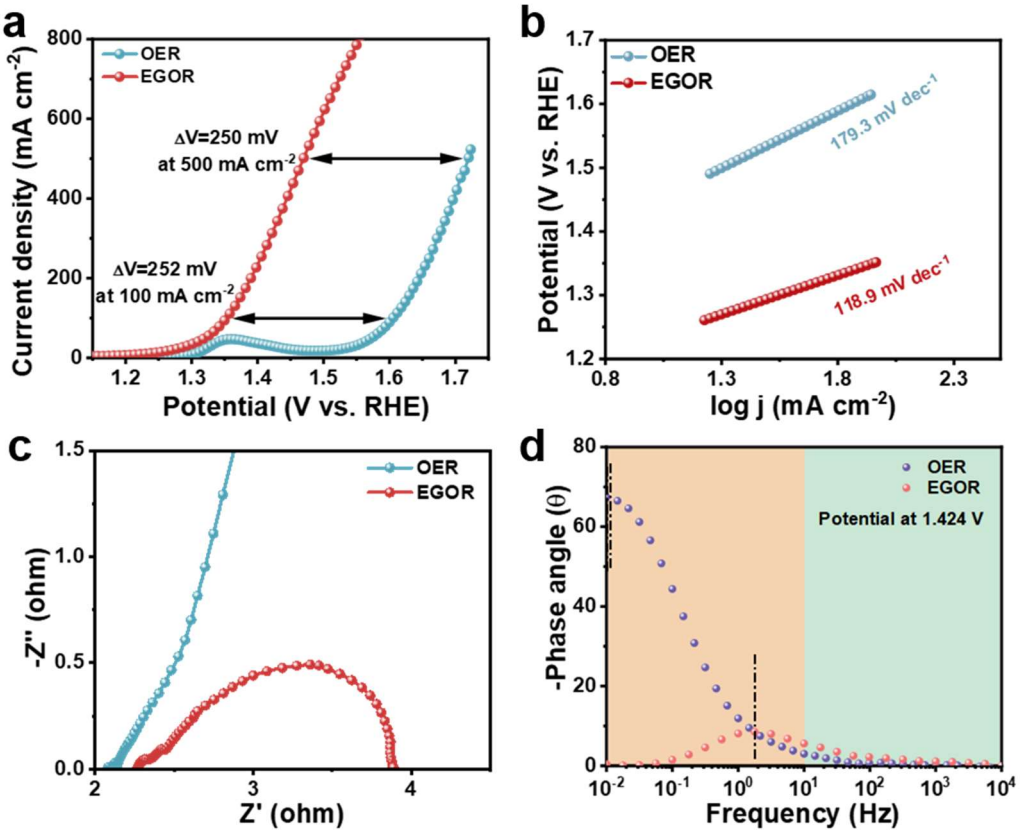

Fig. S14 (a) LSV curves of NiCu-LDH/$NiCo_2O_4$/NF measured in 1 M KOH with and without EG. (b) Corresponding Tafel slope plots for the EGOR and OER processes. (c) Nyquist plots and (d) Bode plots of NiCu-LDH/$NiCo_2O_4$/NF for EGOR and OER.

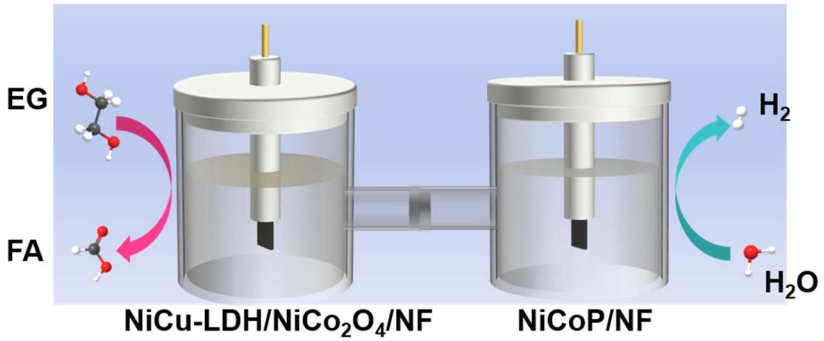

Fig. S15 Schematic illustration of the H-type electrolytic cell.

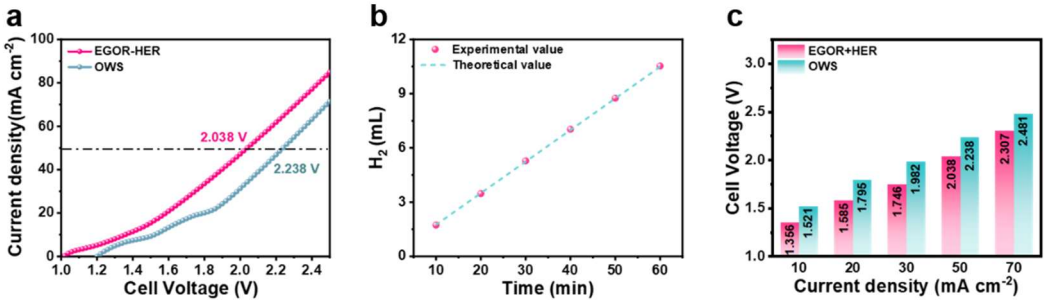

Fig. S16 (a) LSV curves of EGOR–HER system and conventional overall water splitting (OWS) systems. (b) Comparison of theoretical and experimentally measured H_2 production at 50 mA cm^{-2}. (c) Operating voltages at different current densities.

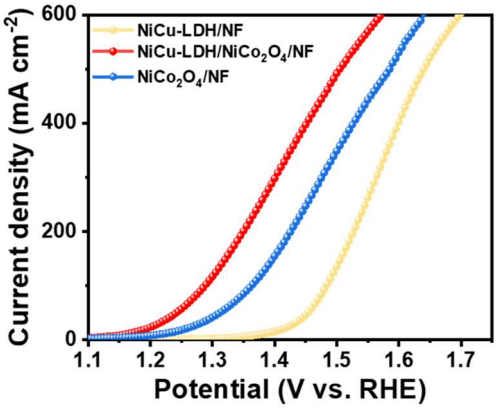

Fig. S17 LSV curves recorded in 1.0 M KOH with 0.5 M glycerol.

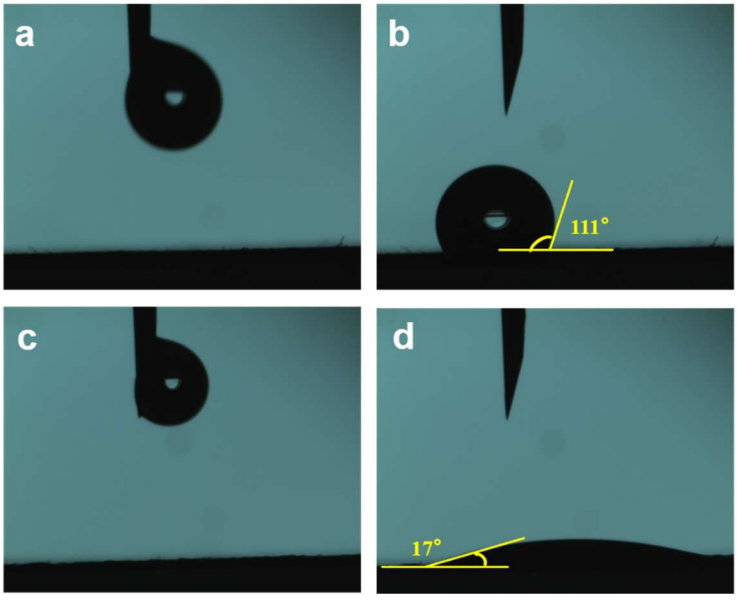

Fig. S18 Water contact angle images of (a, b) Co_3O_4/NF and (c, d) NiCu-LDH/Co_3O_4/NF.

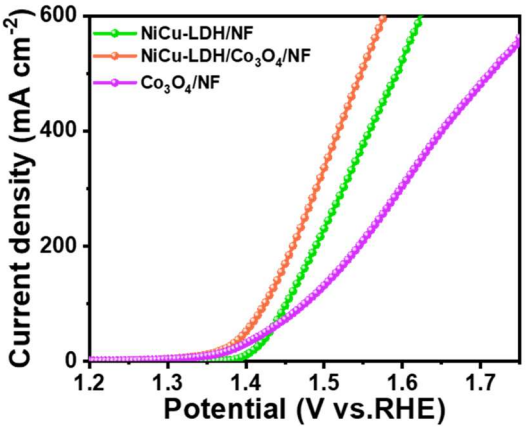

Fig. S19 LSV curves recorded in 1.0 M KOH with 0.5 M EG.

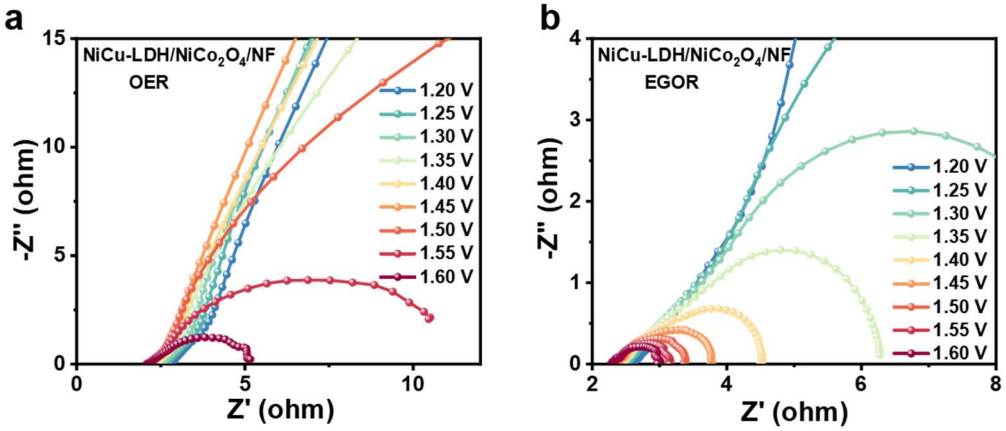

Fig. S20 Nyquist plots of NiCu-LDH/$NiCo_2O_4$/NF for (a) OER and (b) EGOR.

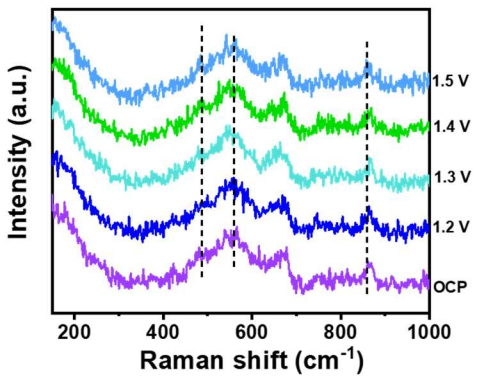

Fig. S21 In situ Raman spectra of NiCu-LDH/$NiCo_2O_4$/NF for EGOR.

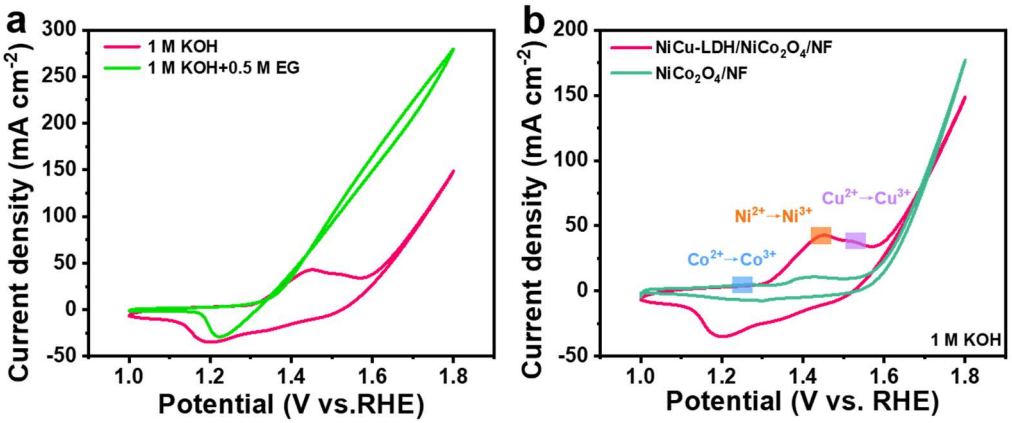

Fig. S22 (a) CV curves recorded at 5 mV s^{-1} for NiCu-LDH/$NiCo_2O_4$/NF in 1 M KOH with and without 0.5 M EG, (b) CV curves for NiCu-LDH/$NiCo_2O_4$/NF and $NiCo_2O_4$/NF in 1 M KOH.

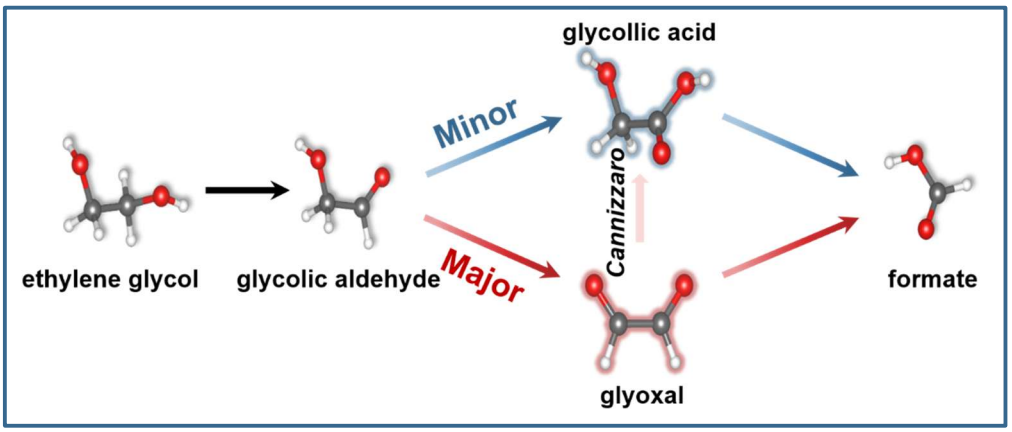

Fig. S23 Proposed reaction pathways for the oxidation of EG to FA.

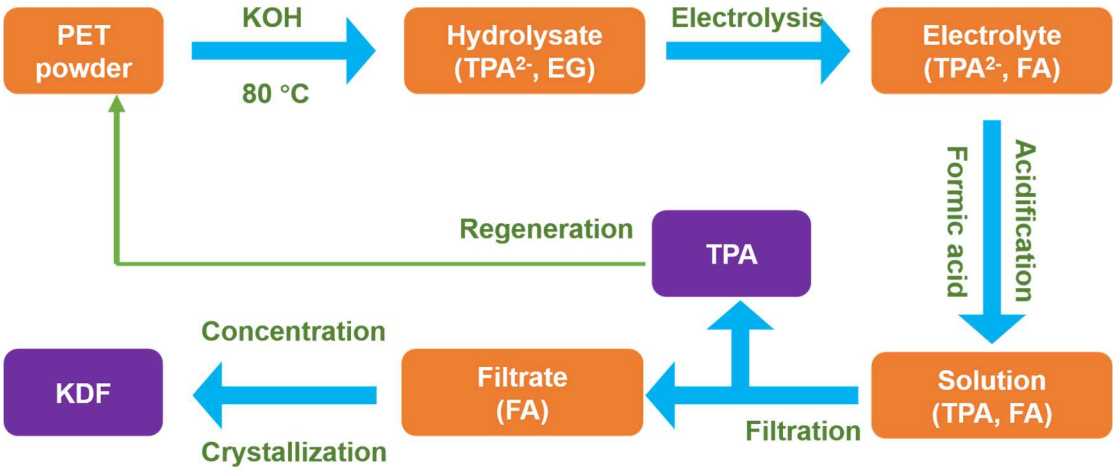

Fig. S24 Schematic illustration of the electrocatalytic PET upcycling to KDF and TPA.

Table S1. Atomic percentages of elements in NiCu-LDH/$NiCo_2O_4$/NF, $NiCo_2O_4$/NF, and NiCu-LDH/NF determined by XPS analysis.

Samples	Ni (%)	Co (%)	Cu (%)	O (%)
NiCu-LDH/$NiCo_2O_4$/NF	6.03	4.91	2.29	31.82
$NiCo_2O_4$/NF	5.56	13.00		44.65
NiCu-LDH /NF	3.40		4.59	22.31

Table S2. A summary of performances of the NiCu-LDH/$NiCo_2O_4$/NF and other recently reported EGOR electrocatalysts.

Catalyst	**Organics**	**Voltage for 100 mA/cm^2 (V)**	**Faraday efficiency**	**Stability**	**Ref.**
NiCu-LDH/$NiCo_2O_4$/NF	1 M KOH with 0.5 M EG	1.35	92.7%	120 h	This work
NiCu60s/NF	1 M KOH with 0.3 M EG	1.45	95.8%	24 h	ACS Catal. 2024, 14, 5314-5325
$Ni_{0.9}Mn_{0.1}$LDH	1 M KOH with 1 M EG	1.65	85.8%	/	Angew. Chem. Int. Ed. 63, 2024, e202411517
$NiCo_2O_4$/CFP	1 M NaOH with 0.1 M PET	1.5	90%	/	ACS Catal. 2022, 12, 6722-6728

	hydrolysate				
AC-NiO/NF	1 M KOH with 0.3 M EG	1.37	80%	10 h	Angew. Chem. Int. Ed. 2024, 64, e202418640
Co_2CuO_4 NWA/NF	1 M KOH with 25 mg/mL PET hydrolysate	1.45	93%	/	Green Chem. 2022, 24, 6571-6577
CuO NWs-200 °C	0.1 M KOH with 10 mM EG	1.45	88%	40 h	J. Phys. Chem. Lett. 2022, 13, 622-627
Co, Cl-NiS	1 M KOH with 0.1 M EG	1.34	93.5%	12 h	Nano-Micro Lett. 2023, 15, 210
ys-ZIF@CoFe-LDH NCs	1 M KOH with 0.5 M EG	1.42	91%	16 h	eScience 2023, 3, 100118
CoO/CFP	1 M KOH with 0.1 M EG	Over 1.60	/	6 h	Adv. Energy Mater. 2023, 13, 2301572
NiFe-sc-PBA	1 M KOH with 1 M EG	1.40	Above 92%	500 h	Nat. Commun. 2025, 16, 3458
Ni300s/NF	1 M KOH with 0.1 M PET hydrolysate	1.40	90%	720 h	Appl. Catal., B. 2025, 371, 125211
Branched $NiSe_2$/C	1 M KOH+1 M EG	1.60	Above 80%	Two days	Adv. Sci., 2023, 10(15):2300841.
Co-ZIF-L/CNQDs	1 M KOH+0.3 M EG	1.50	91.2%	100 h	Appl. Catal. B: Environ. 2026, 385, 126279.
CoPO/C	1 M KOH+0.1 M EG	1.36	93.8%	10 h	ChemSusChem, 2026, 19: e202502167
2D-CoNi-PET	1 M KOH+0.3 M EG	1.41	91%	72 h	Small, 2026, 22, e12758.
NiCo-MOF	1 M KOH+0.5 M EG	1.33	95.6%	50 h	Chem. Eng. Sci., 2025, 317: 122101.
Ni–Co_9S_8 NSAs/NF	1 M KOH+1 M EG	1.28	92%	24 h	J. Mater. Chem. A, 2024, 12(48): 33917-33925.

Ag/NiFe-LDH/NF	1 M KOH+1 M EG	1.47	85%	24 h	Chin. J. Catal., 2026, 80: 282-292.
Ru-Co_3O_4/CF	1 M KOH+0.5 M EG	1.35	91%	120 h	Chem. Eng. J., 2025, 511: 161855.
CoCuOx@MXene/NF	1 M KOH+0.3 M EG	1.41	93.2%	48 h	J. Energy Chem., 2025, 104: 91-100

Economic analysis

To evaluate the economic potential of this electrocatalytic system, we conducted a comprehensive techno-economic analysis (TEA). Firstly, we set up a relatively appropriate technical economic model to evaluate the product profitability.[1,2] In order to better simulate the actual industrial situation, the calculation scope includes PET pretreatment cost, electricity costs, electrolyte and membrane replacement costs, as well as maintenance costs of electrolytic cells, supporting facilities and separation and purification costs. Based on the US Department of Energy's recently announced 2025 utility-scale solar cost target, we estimate the cost of renewable electricity to be 0.03 $/kWh with an electricity conversion efficiency of 90%.[3,4] The specific calculation method is as follows:

Total costs:

1. Raw material cost

$$\text{PET cost} = 100\ \text{ton} \times 390\ \$/\text{ton} \times 350\ \text{day} = 1.365\times10^7\ \$$$

$$\text{KOH cost} = 40\ \text{ton} \times 850\ \$/\text{ton} \times 350\ \text{day} = 1.19\times10^7\ \$$$

$$\text{FA cost} = 92.7\ \text{ton} \times 400\ \$/\text{ton} \times 350\ \text{day} = 1.2978\times10^7\ \$$$

$$\text{Raw material cost} = 38528000\ \$$$

2. Capital cost

Here, the main operating conditions are as follows: Based on our assumption, the production scale is set at 100 tons of PET per day over 350 operating days per year. The service life of the electrolyzer stack is assumed to be 5 years.[5,6] The stack cost is assumed to be 460 $/kW.[7] The reference electrolyzer operates at 1.7 V and 0.196 A/cm^2,

and an installation factor of 1.12 is applied. The balance of plant (BoP) cost is taken as 35 % of the total electrolyzer system cost, values derived from the H2A model. The downstream separation strategy was designed considering the chemical form of the products: both TPA and FA are present as potassium salts. To enable efficient recovery, anhydrous formic acid is employed for pH adjustment. The capital expenditure for product separation and purification is estimated to be 30 % of the raw material cost.[8]

Total current = 9×10^7 g/day ÷ 192 g/mol × 3 × 96485 C/mol ÷88.63% ÷ 86400 = 1771854 A

Electrolyzer area =1771854 A ÷ 0.196 A/cm^2 ÷ 10000 cm^2/m^2 = 904 m^2

Electrolyzer cost = 0.46 $/W × 1771854 A × 1.70 V = 1385590 $

Balance of plant cost = 1385590 $ × 0.35 / 0.65 = 746087 $

Separation cost = 38528000 $ × 30% = 11558400 $

Capital cost = 13690077 $

Operating cost

The working and maintenance cost was assumed to be 2.5% of the capital cost. According to the literature, the catalysts and membrane costs are assumed to be $1,000 per m^2 with the lifetime of 1 years. The nominal interest rate is 7%.[9] As mentioned above, the separation of cathode products need not be considered, but the purification of anode TPA and FA is an energy intensive separation process. Thus, we assume the utilities cost account for 60% of the raw material cost.[10] Given the loss of electrolyte due to neutralization, it is assumed that the consumption cost of electrolyte and water accounts for 30% of the cost of raw materials.

The capital recovery factor (CRF): $CRF_{\text{catalysts and membrane}} = i(1+i)^{\text{lifetime}}/[(1+i)^{\text{lifetime}} -1] =1.07$

Catalysts and membrane cost = electrolyzer area × catalysts and membrane cost per square meter × $CRF_{\text{catalysts and membrane}}$ = 904 m^2 × 1000 × 1.07 = 967280 $

Electricity cost = 1771854 A × 1.7 V × 24 ÷ 1000 × 0.03 $/kWh × 350 day = 759062 $

Working and maintenance cost = 9837277 $ × 2.5% = 245931 $

Cost of liquid separation = 38528000 $ × 60% = 23116800 $

Water and electrolyte cost = 38528000 $ × 30% = 11558400 $

Operating cost =36647473 $

Other cost

Other cost, such as operating overhead, labor-related cost and selling (or transfer) expense, account for 20% of the cost of raw materials

Other cost = 38528000 $ × 20% = 7705600 $

Product value

Based on market prices and literature references, the selling prices of TPA, KDF and H_2 are set at 1590 $/ton, 7210 $/ton,[11] respectively.

TPA sales = 84.1 ton × 1260 $/ton × 350 day = 37088100 $

KDF sales = 113 ton × 1590 $/ton × 350 day = 62884500 $

H_2 sales =1.5 ton × 7210 $/ton ×350 day = 3785250 $

Product value = 103757850 $

Total profit

Therefore, the profit per year of electrolysis of PET can be calculated:

Total profit = 7186700 $/year = 205.33 $/$ton_{PET}$

1 J. Qi, Y. Du, Q. Yang, N. Jiang, J. Li, Y. Ma, Y. Ma, X. Zhao and J. Qiu, *Nat. Commun.,* 2023, **14**, 6263.

2 L. Ma, Y. Miao, J. Yang, Y. Fu, Y. Yan, Z. Zhang, Z. Li and M. Shao, *Adv. Energy Mater.,* 2024, **14**, 2401061.

3 N. M. Haegel, R. Margolis, T. Buonassisi, D. Feldman, A. Froitzheim, R. Garabedian, M. Green, S. Glunz, H.-M. Henning, B. Holder, I. Kaizuka, B. Kroposki, K. Matsubara, S. Niki, K. Sakurai, R. A. Schindler, W. Tumas, E. R. Weber, G. Wilson, M. Woodhouse and S. Kurtz, *Science,* 2017, **356**, 141-143.

4 M. Jouny, W. Luc and F. Jiao, *Ind. Eng. Chem. Res.,* 2018, **57**, 2165-2177.

5 H. Lee, S. Kwon, N. Park, S. Cha, E. Lee, T. H. Kong, J. Cha, Y. Kwon, *J. Am. Chem. Soc. Au,* 2024, **4**, 3383-3399.

6 J. Vos, A. Ramírez and M. Fortes, *Renew. Sustain. Energy Rev.*, 2025, **213**, 115454.

7 H. Shin, K. U. Hansen, F. Jiao, *Nat. Sustain*., 2021, **4**, 911-919.

8 Z. Wang, Y. Wang, J. Chen, H. Yu, Y. Xu, K. Deng, H. Wang and L. Wang, *J. Mater. Chem. A*, 2025,**13**, 20439-20446.

9 X. Wang, Y. Chen, F. Li, R. K. Miao, J. E. Huang, Z. Zhao, X.-Y. Li, R. Dorakhan, S. Chu, J. Wu, S. Zheng, W. Ni, D. Kim, S. Park, Y. Liang, A. Ozden, P. Ou, Y. Hou, D. Sinton and E. H. Sargent, *Nat. Commun.,* 2024, **15**, 616.

10 J. Na, B. Seo, J. Kim, C. W. Lee, H. Lee, Y. J. Hwang, B. K. Min, D. K. Lee, H. S. Oh and U. Lee, *Nat. Commun.,* 2019, **10**, 5193.

11 F. Liu, J. Zhou, X. Gao, R. Shi, Z. Guo, E. Tse and Y. Chen, *Angew. Chem. Int. Ed,* 2025, **64**, e202422183.